

(Draft of 4/7/09)

Some hidden physiology in naturalistic spike rasters. The faithful copy neuron.

Brain Connectivity Workshop

Sydney, June 13, 08. Bruce Knight

Abstract

Certain biophysically plausible specializations can endow the performance of a population of neurons with a remarkably convenient property – the “faithful copy” property – which reveals itself when such a neuron yields a spike raster in response to repetition of a naturalistic stimulus. Below I’ll explore 3 major points. (1) Some of a model neuron’s parameters carry the physical dimension of rate (sec^{-1}) and if these should be combined with a time-course proportional to that of the neuron’s synaptic input current then the faithful copy property results. (2) We may conjecture, on the basis of familiar evolutionary argument, that in some common neuron applications survival pressures should favor such designs. We may look for evidence of this in laboratory data. (3) Given a raster of spike-time data from a repeated naturalistic stimulus, we may construct a new “clock” whose “revised time” counts (instead of seconds) the advancing expected number of spike events consequent to the irregular naturalistic input. A neuron which has the faithful copy property reveals that feature by producing, under this revised clock, a single universal interspike-interval histogram which always emerges even across separate epochs where the firing rate is slow, or is fast, or is rapidly changing*. Some real neurons yield spike rasters which come close to this result, and such neurons may be reasonably modeled from this data analysis.

* Early development of much of this idea, together with analysis of laboratory data, is given in Reich *et al.* (1998).

If we decide to take a hard theoretical look at a part of the brain, to try and figure out how its dynamics unfolds as time progresses, then one very natural early step we can make is to conceptually divide the brain into sub-populations (perhaps numerous sub-populations) of neurons, where we insist that all the member neurons of each sub-population are closely similar in design and also that they all are activated by closely similar synaptic inputs.

Now a natural output variable to inspect in a large homogeneous population of neurons, is the whole population's aggregated nerve-impulse firing rate. This clearly important dynamical variable, when analyzed in terms of causal input-output relations, has one quite unusual and surprising property. In most precisely defined dynamical systems which have at least a few internal degrees of freedom, there is a quantifiable "hesitation tendency" between change in input and consequent change in output. Not so for the large population firing response; within a large population of neurons there are always members which are at the verge of firing, and their rate of threshold-crossing responds at once to a change in input. This feature is solidly confirmed both by theory and by computer simulation.

When we undertake a detailed theoretical examination of neuron population dynamics, this surprise leads to another pleasant surprise: within the set of neuron models which are defined by our equations, if we exercise enough care we can choose a subset of models for which the immediate part of the response is the whole story. That is to say, it is possible to choose mathematical neuron models which have the feature that the time varying synaptic input current for the whole population, and the whole population's consequent firing rate, are in a fixed ratio. For such a model neuron population, every time-varying feature of input current is exactly mimicked by the population's firing rate. I'll refer to such model neurons as "faithful copy" neurons. Again, simulations

strongly confirm this property. And if someone asks a question, at the end I'll work out some brief mathematics.*

So we have our part of the brain conceptually divided into homogeneous sub-populations. If each sub-population is composed of faithful copy neurons, then we discover that it is not an overwhelming challenge to interconnect those sub-populations in ways that will flexibly perform brain-like tasks. For example, let's connect two layers, each a set of such sub-populations, in a simple feed-forward manner, with every member of the second layer targeted by inputs of various weights from different members of the first layer. We can arrange the interconnection weights to fulfill the following non-trivial task which we might call "pattern identification". Let us choose a set of specific alternative patterns of relative activity which may appear across the sub-populations of the first layer. Then it is a fairly straightforward matter to choose the interconnection weights in such a way that, when each different pattern appears across the first layer, it causes responsive firing activity only in one corresponding different sub-population in the second layer. The identity of the uniquely active second sub-population specifies which pattern has appeared across the first set. Again, in response to a question, I'll give the brief rule for choosing the weights of the interconnections.*

Now suppose that, into the synapses of the first layer, we input a superposition of two of our patterns at intensities with two separate time courses. Both of the two appropriate output channels will respond, each with its own appropriate time course of activity, and without cross-talk between the channels.

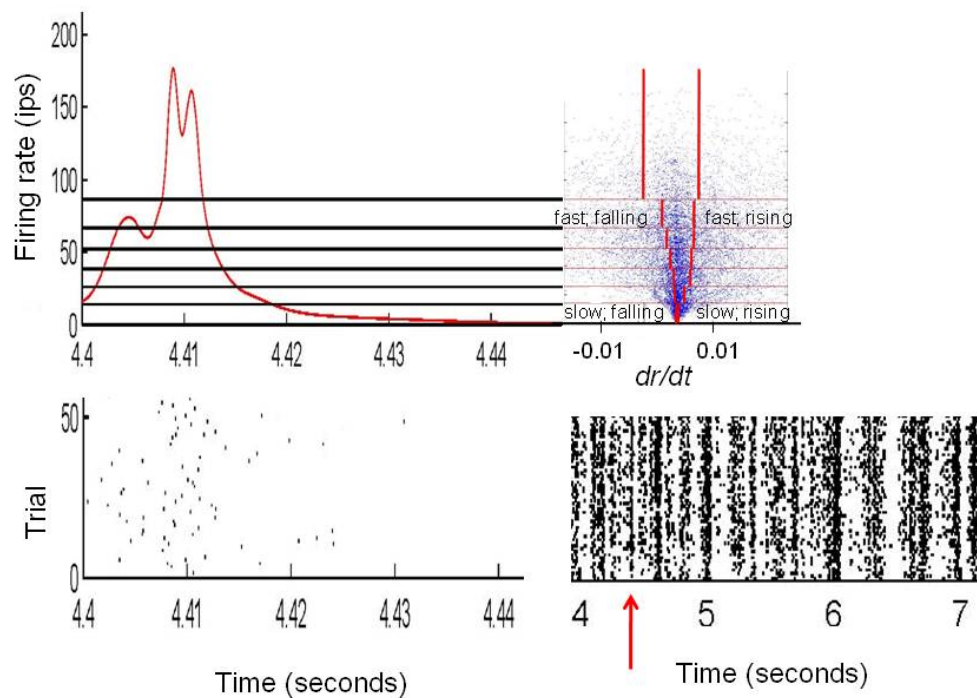
* See Appendix 1.

* See Appendix 2

That's just one example of what can be done with faithful copy neurons. We may suspect that evolutionary pressures might select for something like these specialized designs. So here's a procedure that might help us to find out, whether such selection has in fact taken place.

[Slide 1].

A. Casti, M. Crumiller, P. Shirvalkar, L. Sirovich, & E. Kaplan



RGC: spot size=160 (June 22, 2005)

In the lower right frame we see part of a spike raster generated by repeated presentations of a naturalistic stimulus. An outline of our data analysis will proceed from that raster clockwise to the upper right frame.

First my colleagues, all of whom are at the Mount Sinai School of Medicine in New York.

Alex Casti is an Assistant Professor working with Udi Kaplan. Together with Udi, Alex has done a long series of experiments, of which this is one. Alex also did a lot of relevant programming. Marshall Crumiller and Prasad Shirvalkar are two starting PhD candidates who have done much of the heavy lifting in programming; in large part this has been a learning experience for them. Larry Sirovich is not only a long-time theoretical and experimental neuroscientist, he is a foremost expert in applied asymptotic analysis and has published an advanced text on the topic. His asymptotic analysis will be applied later to the next slide.

We can ask: how can you extract a quantitative neuron model from a raster generated by repeating a messy naturalistic stimulus? Here's how; this will give us some valuable quantitative characterization, quite aside from any questions about whether our neuron has the faithful copy property. But if it does, that property will leap out at us.

Our stimulus derives from one of the van Hateren stimuli off the internet. Van Hateren documented the prowling of a cat through his shrubbery and followed the same course with a video camera. The video is 8 seconds long of which we see about 3 seconds here with spikes recorded from a retinal ganglion cell of an anesthetized cat. We see about 50 of the 128 trials and the full record contained about 21,000 nerve impulse events.

In the lower left frame, we have simply expanded the time scale by about a factor of 100, to resolve detail in the typical feature which is marked by the red arrow.

Now if we have repeated samples of a stochastic point process in time, and if we merge the events in those repeats to a single time-line,

we don't have to merge a lot before our merged record approaches a typical sample of an inhomogeneous Poisson process. An inhomogeneous Poisson process is characterized by an underlying continuous rate function in time. With a sample of the inhomogeneous Poisson process on hand we may apply statistical procedures to approximately extract a maximum-likelihood estimate of that continuous rate function*. The raster of events in the lower left frame we have merged to a single time line, and the red curve in the upper left frame is their estimated rate function.

Now to every spike event, such as those which we see in the lower left frame, we can naturally assign a value of the rate function which we have found, and to the same event we also can assign a value of the speed at which that rate function is changing. In the slide's upper right frame we have plotted those two variables for each of almost all of our roughly 21,000 spike events.

In the upper right frame our spike events are ordered vertically according to the size of their rate function, and we have divided them into seven equally numerous sets of about 3,000 events each. Then we have subdivided each of these sets into three equally numerous subsets of about 1,000 each, according to how rapidly their rate function is rising or is falling.

Now a function of time, such as our rate function, which not only has bounded variation but also moves smoothly, must spend a good deal of its time not moving very rapidly. We verify this by noting that each box in the middle set (which boxes hold $\frac{1}{3}$ of our spike events) doesn't occupy much of the full horizontal spread over which these events can range. We also note that within each of the central 5 of our 21 boxes,

* Our procedure is given in the website reference Knight (2008). This is a development of Reich *et al.* (1998)

the events are fairly homogeneously distributed. We can exploit that feature for further analysis of our data.

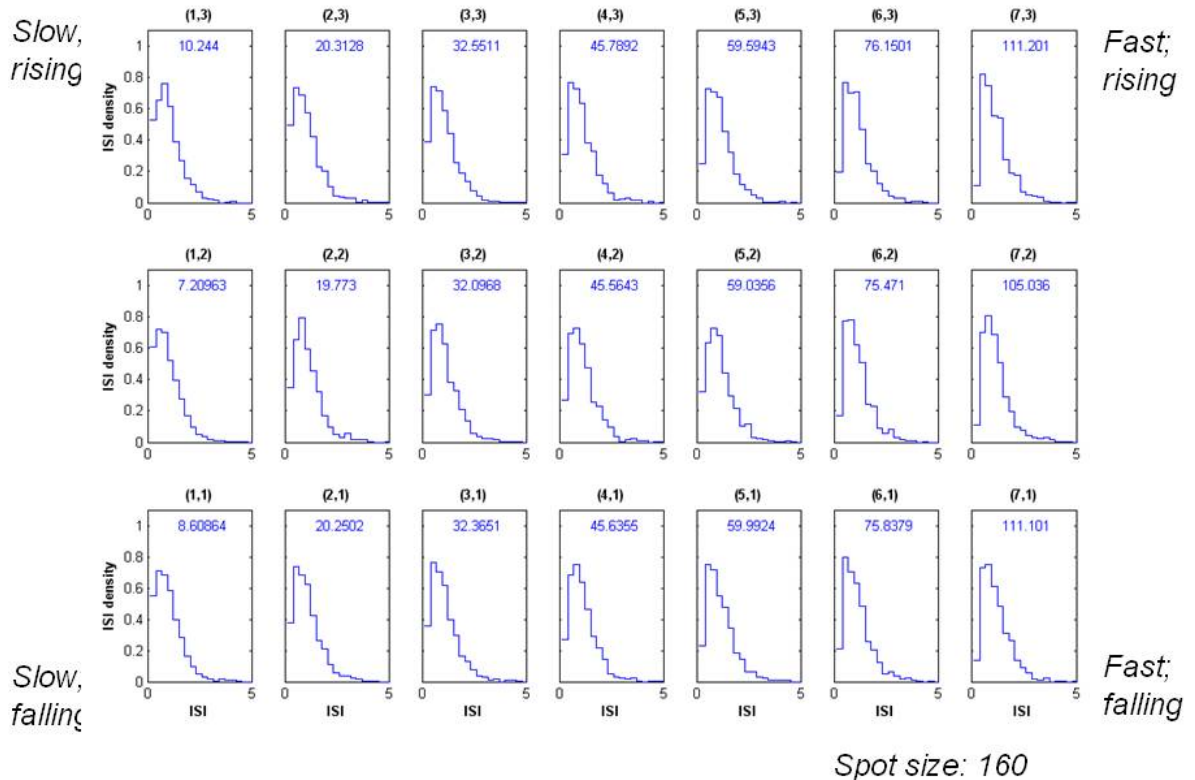
We observe that a neuron contains several internal processes each of which carries its own time-scale. When the neuron fires fast or slow, do these processes re-balance with respect to one another? Our data may address this: in any one of our 5 central boxes, each one of the 1,000 events has a predecessor, and this enables us to construct an interspike-interval histogram for each box; by comparing the results from the different boxes, we may see whether a change in the mean rate induces a change in the histogram's shape.

To do this systematically, we must establish a common time-scale for our histograms; for each histogram we must express time in terms of the mean interpulse time. A sensible way to achieve this at a single blow is to make a transformation from laboratory time to a new "revised time" variable whose rate of advance is always given by the height of the red rate curve which we developed in the upper left frame. That is to say, at any laboratory time our "revised time" clock always reads out the accumulated area to the left under the red curve. For each trial on our raster, we will measure interspike intervals in this revised time.

This somewhat elaborate preparation has an additional payoff. Suppose our neuron has the faithful copy property. Then it is easy to show that, aside from noise, the histograms in all 21 of our boxes should be the same. Here's what the laboratory data say.

[Slide 2]

Interval histograms at various firing rates



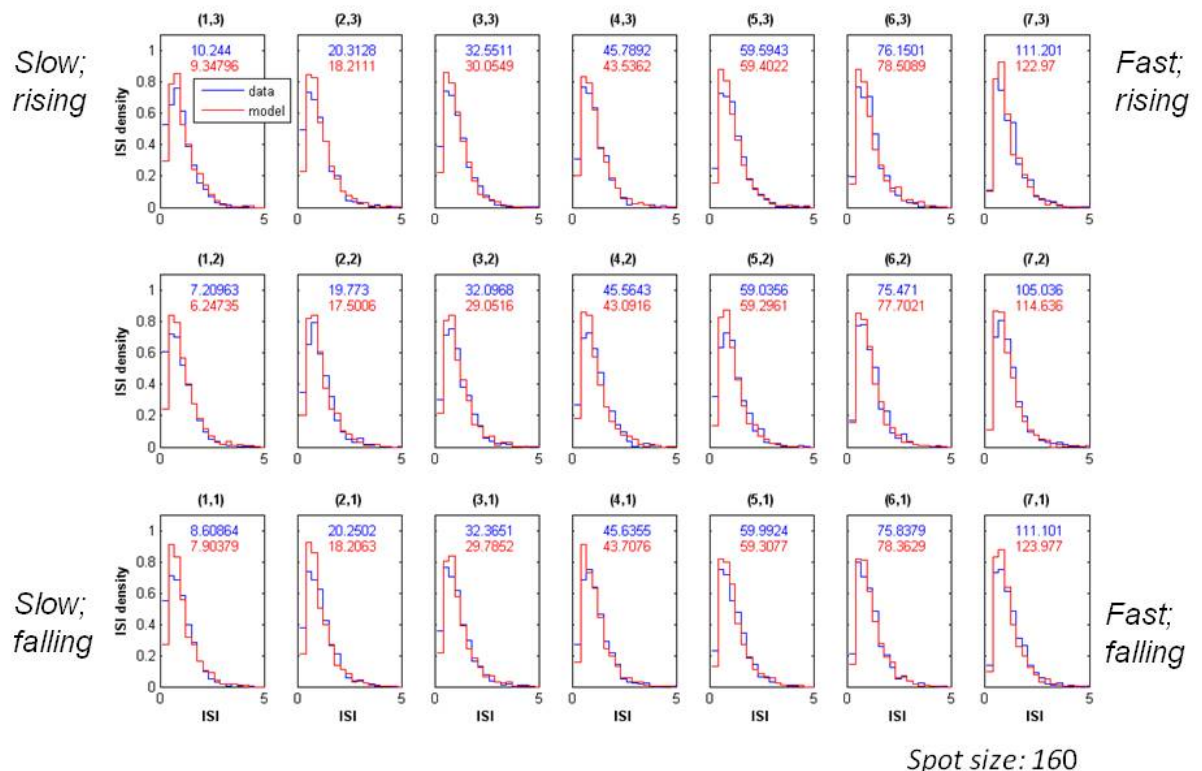
Here the 7 different mean rates are spread out horizontally. The histograms for the 5 central boxes, where firing conditions were quite homogeneous, are central in the middle row, indexed (2, 2) through (6, 2). The mean rates run from about 10 events per second on the left to more than 100 per second on the right. The most striking feature here is the great similarity of all these histograms, which suggests that the performance of our retinal ganglion cell was close to that of an idealized faithful copy neuron. Across the five histograms that correspond to clean homogeneous conditions, we do see a visible small trend toward a more pronounced early dead-time as mean rate increases. This trend is

echoed in the other two rows of very similar histograms which represent unsteady conditions where the mean rate is rising or falling.

This small trend in the 5 central histograms encourages us to fit these data with a 4-parameter neuron model which departs a bit from the faithful copy condition. Our model is essentially a noisy and leaky integrate-and-fire neuron model in which both diffusion and membrane leakage are linear functions of synaptic current but with non-zero offsets at zero current. We have simulated the same experiment with our model, and a comparison with the real neuron is shown on the last slide*.

[Slide 3]

Interval histograms at various firing rates



* See appendix 3.

Again we see something near the faithful copy property, with a small trend in dead-time. In contrast, the commonly employed model noisy and leaky integrate-and-fire neuron, with constant leakage coefficient and constant diffusion, for the central 5 histograms at the specified rates, would yield quite different histograms with pronounced systematic trends.

In summary, data from some real neurons show something close to the faithful copy condition, which condition greatly simplifies Mother Nature's challenge in appropriately connecting brain regions for the production of brain-like behavior. If we collect from such a neuron a spike raster in response to a repeated naturalistic stimulus, there is present indication that this may enable us to simulate that neuron well with a fairly simple model.

Appendix 1

For a wide set of neuron models which are defined in terms of internal parameters, it is straightforward to first realistically generalize to models where these parameters are replaced by functions of time and then specialize to examples which have the faithful copy property. We illustrate with the leaky and noisy integrate-and-fire neuron model, which combines simplicity with features of useful generality. The simple leaky integrate-and-fire model without noise may be defined by

$$\frac{dx}{dt} = s(t) - \gamma x, \quad x = 1 \rightarrow x = 0, \quad (1.1)$$

where x is transmembrane voltage normalized by the firing threshold voltage (whence x is a physically dimensionless representation of intracellular voltage), γ is the ohmic relaxation rate (with physical dimension $(\text{time})^{-1}$) and the synaptic input current $s(t)$ in this normalization likewise is dimensionally a rate.

Equation (1.1) gives rise to the leaky and noisy integrate-and-fire model if a stochastic fluctuation term is added to the causal $s(t)$. This more general situation is conveniently described

in terms of the time-dependent probability density distribution over voltage $\rho(x,t)$ which satisfies the master equation

$$\frac{\partial \rho}{\partial t} = \frac{\partial}{\partial x} \left\{ -(s(t) - \gamma x) \rho + D \frac{\partial \rho}{\partial x} \right\}, \quad (1.2)$$

where the new feature of stochastic fluctuation is taken into account by the appearance of the diffusion coefficient D (likewise a rate, as x is dimensionless). The threshold reset condition expressed in equation (1.1) demands the boundary condition that

$$\rho(1,t) = 0. \quad (1.3)$$

The form of (1.2) leads us to define the probability current

$$J(x,t) = (s(t) - \gamma x) \rho - D \frac{\partial \rho}{\partial x} \quad (1.4)$$

which, by (1.2), satisfies the continuity equation

$$\frac{\partial \rho}{\partial t} + \frac{\partial J}{\partial x} = 0. \quad (1.5)$$

The threshold reset condition requires that

$$J(0,t) = J(1,t) \quad (1.6)$$

(a second boundary condition for (1.2)), whereupon integrating (1.5) over the range of x demonstrates that total probability is conserved. The structure of the master equation (1.2) is such that in the special case where s is in fact a time-independent constant we may start with an arbitrary initial condition $\rho(x,0)$ and it will relax to a time independent steady state

$$\rho(x,t) \rightarrow \rho_0(x) \quad (1.7)$$

for which we may solve by setting $\partial \rho / \partial t$ to zero in (1.2).

Now in real neurons intracellular noise fluctuations include synaptic noise which changes with input current, and it is commonly seen in the laboratory that transmembrane resistance decreases with increasing firing activity. So it is natural to generalize (1.2) to

$$\frac{\partial \rho}{\partial t} = \frac{\partial}{\partial x} \left\{ -(s(t) - \gamma(t)x) \rho + D(t) \frac{\partial \rho}{\partial x} \right\} \quad (1.8)$$

Under this generalization, the current (1.4), boundary conditions (1.3) (1.6), continuity equation (1.5), and conservation of total probability all remain intact. The set of neuron models (1.8) is far broader than is (1.2) where γ and D are constant, and is rather inexplicitly broader as the definitions of the functions of time $\gamma(t), D(t)$ have been left open.

We may now specialize to a set of neuron models which have the faithful copy property.

Let

$$\gamma(t) = \alpha s(t) \quad (1.9)$$

$$D(t) = \beta s(t) \quad (1.10)$$

where the values of the dimensionless constants α and β have still been left open. We comment that if intracellular fluctuations are dominated by synaptic shot noise then (1.10) follows quite naturally (see Knight, Manin, and Sirovich (1995)), while an effective ohmic leakage of the form (1.9) would require some discrimination in choosing the dynamics of voltage-dependent transmembrane ionic channels.

Substitution of (1.9), (1.10) into (1.8) gives the more specialized equation

$$\frac{\partial \rho}{\partial t} = s(t) \frac{\partial}{\partial x} \left\{ -(1 - \alpha x) \rho + \beta \frac{\partial \rho}{\partial x} \right\}. \quad (1.11)$$

This neuron population master equation has the faithful copy property, as we now show. If we define, as an alternative to time, a new variable

$$\hat{t}(t) = \int_0^t dt' s(t') \quad (1.12)$$

then

$$dt = \frac{1}{s(t)} d\hat{t} \quad (1.13)$$

and substitution into (1.11) gives

$$\frac{\partial \rho}{\partial \hat{t}} = \frac{\partial}{\partial x} \left\{ (-1 + \alpha x) \rho + \beta \frac{\partial \rho}{\partial x} \right\}. \quad (1.14)$$

The right-hand-side of this equation is now independent of \hat{t} and, just as we saw above for equation (1.2) when s was a time independent constant, the solution $\rho(x, \hat{t})$ of (1.14) relaxes to a function of x independent of \hat{t} :

$$\rho(x, \hat{t}) \rightarrow \rho_0(x) \quad (1.15)$$

where again we may determine $\rho_0(x)$ by setting the time derivative to zero in (1.14) and then solving the linear homogeneous ordinary differential equation. As what we have done here followed from equation (1.11), clearly (1.15) must solve (1.11) as well.

Now the population firing rate, reduced to a per-neuron basis, is the same as the probability current for a neuron crossing the firing threshold at $x = 1$, and because of the boundary condition (1.3), substitution back into the expression for current (1.4) gives us the firing rate

$$r(t) = J(1, t) = s(t) \left(-\beta \frac{d\rho_0(x)}{dx} \Big|_{x=1} \right). \quad (1.16)$$

Because the probability density, which necessarily is not negative, descends to zero at $x = 1$, the derivative of ρ_0 at that point is negative, and (1.16) is positive, as it should be. Now note that the firing rate (1.16) is in fixed ratio with the synaptic input $s(t)$. This is the faithful copy property.

This remarkable property follows from the choices of time-dependence (1.9), (1.10) which led to a probability density over state-space (1.15) which did not have to re-balance in

response to changes in input. The availability of such choices is general and not a feature special to this particular type of neuron model.

We note that from the laboratory the firing rate is a directly measurable variable (see main text) while the synaptic input current is not. However, insofar as we can use a model as a guide, if the faithful copy property holds then the input current can be deduced from the firing rate, as in our case

$$s(t) = (-\beta\rho'_0(1))^{-1} r(t). \quad (1.17)$$

Finally, the considerations above lead us to the universal histogram feature which gives a laboratory test, of a recorded neuron, for the faithful copy property. We may study the probability distribution of our neuron's first passage through threshold, which, under steady conditions and in the limit of many passages, is the same thing as the interspike-interval histogram.

The machinery above addresses this task once we remove the return-from-threshold boundary condition (1.6) and allow the neuron to get lost when it reaches $x = 1$. We replace (1.6) with the simpler condition that the probability current must vanish at the leftmost extreme of x . Under these conditions our total probability, that our neuron has not yet reached threshold, relaxes from an initial value of unity, eventually to zero. The momentary rate of decrease of that probability is given by the probability current at $x = 1$. If we start from a spike event with probability unity concentrated at $x = 0$, and follow the solution of (1.8), this probability current, as a function of time, directly traces the momentary likelihood of the next spike occurrence.

Now if we make the faithful copy specializations (1.9), (1.10) we see that in our new time-like variable (1.12) our probability density satisfies the autonomous equation (1.14). In terms of this new variable \hat{t} it does not matter at what time \hat{t}_0 we launch our concentrated probability density

$$\rho(x, \hat{t}_0) = \delta(x); \quad (1.18)$$

equation (1.14), because it is autonomous, will yield the single universal threshold current

$$J(1, \hat{t} - \hat{t}_0) \quad (1.19)$$

which traces out the universal profile of the interspike-interval histogram in the variable \hat{t} .

It is worth observing one detail in conclusion of this appendix. The revised time of the main text is given formally by

$$\tilde{t}(t) = \int_0^t dt' r(t') \quad (1.20)$$

where $r(t)$ is the expected population firing rate on a per-neuron basis, derived directly from a laboratory spike-raster without regard to the question of the faithful copy property. The revised time (1.20) was chosen for the specific reason that across any epoch where r is substantially constant, interspike intervals in the \tilde{t} variable will yield a histogram with a standardized mean value of unity. In case we have a faithful copy neuron which fits the model given above, we can get to the natural time-like variable \hat{t} by using (1.17) in (1.20):

$$\hat{t} = (-\beta\rho'_0(1))^{-1} \tilde{t}. \quad (1.21)$$

The constants β and $-\rho'_0(1)$ are fully specified by the specification of the faithful copy model (equations (1.9), (1.10)).

Appendix 2

We have two sets of faithful copy neuron sub-populations. Each member of the second set receives weighted inputs from members of the first set. The members of each set we can number 1 through N . Each member of each set has a momentary per-neuron firing rate. We will call the firing rate of the q^{th} member of the first set u_q and that of the p^{th} member of the second set v_p . It's natural to refer to the 2 sets as the “ u ” set and the “ v ” set. Because all the neuron sub-populations have the faithful copy property, if synapses respond essentially linearly (which is not biophysically difficult to achieve) then the rate in a member of the second set is determined by those in the first by a relation of the form

$$v_p = \sum_{q=1}^N a_{pq} u_q \quad (2.1)$$

where the a_{pq} may be regarded as the connection weights from the members of the “ u ” set to those of the “ v ” set. It is natural to express the full range, over p , of the relations (2.1), in the vector form

$$\mathbf{v} = A\mathbf{u} \quad (2.2)$$

where the matrix A is formed of the weightings in (2.1).

The challenge in the main text is to pick the weightings A in such a way that they perform a pattern identification. Namely, given for the “ u ” set a list of specific activity patterns $\mathbf{u}^{(1)}, \mathbf{u}^{(2)}, \dots, \mathbf{u}^{(N)}$ of which for example the second is

$$\mathbf{u}^{(2)} = \begin{pmatrix} u_1^{(2)} \\ u_2^{(2)} \\ u_3^{(2)} \\ \vdots \end{pmatrix}, \quad (2.3)$$

to pick the weightings in A such that in this example

$$A\mathbf{u}^{(2)} = \mathbf{v}^{(2)} = \begin{pmatrix} v_1^{(2)} \\ v_2^{(2)} \\ v_3^{(2)} \\ \vdots \end{pmatrix} = \begin{pmatrix} 0 \\ 1 \\ 0 \\ \vdots \end{pmatrix} \quad (2.4)$$

and in general the function of the network is such that when it acts on the k^{th} pattern of u -activities, $\mathbf{u}^{(k)}$, then among the v sub-populations only the k^{th} sub-population is activated, and thereby it identifies the present activity as that of the k^{th} pattern.

As a preliminary we observe that the inverse problem of finding the matrix of weightings B which performs the inverse mapping

$$B\mathbf{v}^{(k)} = \mathbf{u}^{(k)} \quad (2.5)$$

from the single-non-zero-entry vectors (2.4) to the specified set of patterns, is immediately solved by

$$B = (\mathbf{u}^{(1)}, \mathbf{u}^{(2)}, \dots, \mathbf{u}^{(N)}). \quad (2.6)$$

In our example of $k = 2$ we see directly

$$B\mathbf{v}^{(2)} = \begin{pmatrix} u_1^{(1)} & u_1^{(2)} & \dots \\ u_2^{(1)} & u_2^{(2)} & \dots \\ \vdots & \vdots & \dots \end{pmatrix} \begin{pmatrix} 0 \\ 1 \\ \vdots \end{pmatrix} = \begin{pmatrix} u_1^{(2)} \\ u_2^{(2)} \\ \vdots \end{pmatrix}. \quad (2.7)$$

So long as no one of the activity patterns $\mathbf{u}^{(k)}$, which we specified, is a weighted combination of the others, there is a standard procedure to find the inverse

$$A = B^{-1} \quad (2.8)$$

which gives us the set of weightings which solve our pattern identification problem (2.4).

Numerous challenges in brain function are embellishments of this one. In the absence of the faithful-copy specialization, the simple mathematical machinery above becomes unavailable, and because the dynamical equations of neuron electrophysiology are highly nonlinear, strategies for recruiting neuron populations to do things like pattern identification become far more elusive.

Finally, the special case of $N = 2$ above already is informative. Let

$$\mathbf{u}^{(1)} = \begin{pmatrix} \alpha \\ \beta \end{pmatrix}, \quad \mathbf{u}^{(2)} = \begin{pmatrix} \gamma \\ \delta \end{pmatrix} \quad (2.9)$$

so

$$B = \begin{pmatrix} \alpha & \gamma \\ \beta & \delta \end{pmatrix} \quad (2.10)$$

from which

$$A = B^{-1} = \frac{1}{\alpha\delta - \beta\gamma} \begin{pmatrix} \delta, & -\gamma \\ -\beta, & \alpha \end{pmatrix} \quad (2.11)$$

as multiplication of the two matrices confirms. We note that some of the weightings in A must be negative, which implies a network which has inhibitory synapses as well as excitatory. Now experience dictates that any one real neuron terminates with presynaptic connections which are either all excitatory or all inhibitory but never a mixture of both types, an observation known as ‘‘Dale’s law’’. Dale’s law demands a slightly more elaborate relationship between the mathematical formulation and the underlying electrophysiology. Where we spoke above of single sub-populations of neurons, we now must rather envision pairs of sub-populations, and the two members of each pair distinguished by the opposite signs of their synaptic transmission. In equation (2.11), for example, the negative off-diagonal terms $-\beta$ and $-\gamma$ indicate connection weights from the inhibitory member of the pair of sub-populations.

There are further extensions to the ways in which we may correspond these fairly simple mathematical expressions to the more elaborate demands of physiology. For example in the retina we find paired populations of ganglion cells with finite background firing rate - ‘‘on’’ and ‘‘off’’ ganglion cells with mirror changes in firing rate in response to a common change in input. We may assign a negative sign to the firing rate of the ‘‘off’’ cells before merging the paired firing rates to form an effective mathematical population which, in the faithful copy case, shows the convenient property of a linear response which extends on both sides of the value zero.

Appendix 3

It is an essentially straightforward matter in general to create a neuron model of a noisy-and-leaky-integrate-and-fire type which will closely reproduce the five firing rates and interspike-interval histograms from a raster-generating experiment like that which led to Figure 2. For each firing rate (r) and interpulse-interval distribution we determine the parameters s , γ and D . As the five (r, s) pairs are reasonably closely spaced, we may write an interpolation formula valid across their ranges. From $r(t)$, as in the upper left frame of Figure 1, this gives us the corresponding $s(t)$ across the eight-second time-span. The five (s, γ) and (s, D) pairs likewise enable us to interpolate $\gamma(s)$ and $D(s)$ across their ranges of values. At this point the master equation (1.8) may be further specified to the form

$$\frac{\partial \rho}{\partial t} = \frac{\partial}{\partial x} \left\{ -\left(s(t) - \gamma(s(t))x\right)\rho + D(s(t))\frac{\partial \rho}{\partial x} \right\}. \quad (3.1)$$

This equation tells us the distribution function that we would obtain upon repeatedly integrating many trials of the corresponding stochastic ordinary differential equation (Langevin equation)

$$dx = \left(s(t) - \gamma(s(t))x\right)dt + \left(2D(s(t))dt\right)^{1/2}N(0,1), \quad (3.2)$$

where $N(0,1)$ is a random choice from a normal distribution with mean zero and unit variance. Short time-steps dt in (3.2) produce a direct simulation.

We note that in the special case of the faithful-copy property we may substitute (1.9) (1.10) and (1.13) into (3.2) and obtain

$$dx = (1 - \alpha x)\hat{d}t + \sqrt{2\beta\hat{d}t}N(0,1) \quad (3.3)$$

from which the dependence on the current $s(t)$ has dropped out, leaving us a distribution in x (and parametric in α and β) which is a universal function of \hat{t} . This is in fact a second demonstration of the faithful-copy property.

In the experimental case of Figure 2, the faithful-copy property is almost but not quite realized. Interpolation misses the results (1.9) (1.10) slightly, but a single linear least-squares fit is very good, giving us

$$\gamma(s) = \gamma_0 + \gamma's \quad (3.4)$$

$$D(s) = D_0 + D's \quad (3.5)$$

where the small corrections γ_0 and D_0 give us the small departures from the faithful-copy result which we see in Figure 3. We note that the great similarity of the histograms in the top and bottom rows, where input current was very unsteady and no attempt for a fit was undertaken, is further evidence that both the laboratory neuron and the mathematical model derived from it, responded with performance close to that of a faithful-copy neuron.

Some background references

The references below may be found at the website

<http://camelot.mssm.edu/publications/publications.html>

(click on Bruce Knight)

1. The faithful-copy property. With very little mathematical notation two cases, without and then with random noise are discussed in

B.W. Knight, *J. Gen. Physiol.* Vol. 59, 1972.

In section 2, with a bit of follow-up at equations (4.4) and (4.5). (In the website copy three significant errors have been fixed.)

2. The immediate response feature of the population firing rate is presented under fairly general circumstances, though quite formally, in

B.W. Knight, *Neural Computation*, Vol. 12, 2000.

In section 3 this peculiar feature appears in equation (3.5) and again in (3.9). In both equations one term in perturbed output is in fixed proportion to the perturbed input. It surfaces in the firing rate in equation (3.11). Given a defined dynamical input-output system, the quantifiable “hesitation tendency” appears cleanly in the early part of the impulse-response to small incremental impulses, and the impulse response uniquely determines the system’s frequency response, which in general is naturally a function of frequency. But in a faithful-copy system, sinusoids at all frequencies are transmitted with a single fixed input-output ratio. In the equations just quoted such a frequency-independent input-output term appears, and also as the first term in the deduced frequency response equation (3.23) or (3.25). One can easily see that if our equation (1.11), above, is submitted to the procedures of section (3), this frequency-independent term is the only survivor in the frequency response.

3. The shape of the interspike-interval distribution. When time is scaled in terms of the distribution's mean interval, noisy-and-leaky-integrate-and-fire yields a 2-parameter distribution. A computer-convenient 2-parameter asymptotic formula for this distribution is worked out in L. Sirovich and B. Knight, Spiking Neurons and the First Passage Problem, *Neural Computation* -Submitted 2008.
4. The functional form for $D(t)$ (eq. 1.10) is worked out from a shot-noise model in Knight, B.W., Manin, D. and Sirovich, L. Dynamical Models of Interacting Neuron Populations in Visual Cortex. In: *Symposium on Robotics and Cybernetics; Computational Engineering in Systems Applications*. (Gerf, E.C. ed) Cite Scientifique, Lille, France (1996). Also a very quick derivation from a more general finite-jump master equation is sketched in Knight, B.W., Omurtag, A. and Sirovich, L. The Approach of a Neuron Population Firing Rate to a New Equilibrium: An Exact Theoretical Result. *Neural Computation*, 12:1025-1055 (2000) in the paragraph following eq. (2.16).
5. Reich, D.S., Victor, J.D. and Knight, B.W. The Power Ratio and the Interval Map: Spiking Models and Extracellular Recordings. *J. Neurosci.*, 18(23):10090-10104 (1998).
6. Knight, B. Estimation of Rate Function and Revised Time (2008). See also Reich *et al.* (1998) which achieves substantial success by using the impulse response in the δ -function limit.